Pixel coverage models, segmentation, and feature extraction

Joakim Lindblad

joakim@cb.uu.se

Centre for Image Analysis
Uppsala, Sweden

2011-07-15

Work together with Dr. Nataša Sladoje

SSIP 2011, Szeged

Outline

Introducing myself

Joakim Lindblad

Assistant Professor at the Centre for Image Analysis (CBA)
Swedish University of Agricultural Sciences and Uppsala University
Uppsala, Sweden

M.Sc. in Engineering Physics, Uppsala University, Sweden
Ph.D. in Image Analysis, Centre for Image Analysis, Uppsala, Sweden
Post Doc at British Columbia Cancer Research Center, Vancouver, Canada

Centre for Image Analysis
Swedish University of Agricultural Sciences
Uppsala University

Introducing the topic

- The task of **Image Analysis** is to **extract relevant information from images**.
- **Numerical descriptors**, such as area, perimeter, moments of the objects are often of interest, for the tasks of shape analysis, classification, etc.

The standard image analysis task (and its solution)

1. Sample preparation and Imaging
2. Pre-processing (optional)
3. Segmentation
   - Usually crisp
4. Feature extraction
   - Discrete representation problematic
5. Classification, statistical evaluation, . . .

Introducing Fuzzy

- Do not throw away information by making crisp decisions.
- A **fuzzy** approach takes a more nuanced view, allowing preservation of more information.
- A representation based on **fuzzy sets** may may provide numerical descriptors with **higher precision** than what can be achieved from a crisp representation.

The image analysis task and its fuzzy solution

1. Sample preparation and Imaging
2. Pre-processing (optional)
3. Segmentation
    - Fuzzy segmentation (a lot of freedom)
4. Feature extraction
    - Fuzzy representation provides robustness and precision
    - Not always easy to interpret the results; different meanings of memberships
5. Classification, statistical evaluation, . . .

Introducing The Coverage Model

- Keep good sides of fuzzy; stay close to the digital image, high information content, soft boundaries, robustness.
- Restrict to one single meaning of memberships; clear unique interpretation, enabling theoretical results on error bounds.

The image analysis task and its pixel coverage solution

1. Sample preparation and Imaging
2. Pre-processing (optional)
3. Segmentation
   - Pixel coverage segmentation (restricted freedom)
4. Feature extraction
   - Features of the coverage representation
   - Easy to interpret the results, robustness and precision
5. Classification, statistical evaluation, . . .

The Pixel Coverage Model

- The fuzzy framework is very powerful.
- Images contain discrete representations of real continuous objects.
- Our aim is usually to obtain information about continuous real objects, having available their discrete representations.

Pixel coverage digitization

Let the value of a pixel be equal to the part of it being covered by the image object.

- A useful representation that stays close to the original image data.
- Is based on very weak assumptions about the imaged objects.
- Utilizing the coverage information, significant improvement in precision of extracted feature values can be reached.

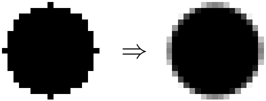

Some background

We are not first ones to work with mixed/partially covered image elements.

- Features directly from grey-level images
  - “Grey levels can improve the performance of binary image digitizers” - N. Kiryati and A. Bruckstein, 1991.
  - Work of Eberly and Lancaster, 1991, and Verbeek and van Vliet, 1993, on grey-level information for length estimation
  - Surprisingly few followers. A problematic dependence between imaging method and feature extraction.
- “Mixed pixels” - satellite imaging (soft classification)
- “Partial volume effects” - tomographic imaging

- Fuzzy segmentation techniques – The Coverage model is a special case of the more general Fuzzy model

- The presented pixel coverage model assumes **crisp** objects.
- The membership of a pixel has a precisely defined meaning.

Pixel coverage digitization

Let a square grid in 2D be given. The Voronoi region associated to a grid point $(i,j) \in \mathbb{Z}^2$ is called pixel $p_{(i,j)}$.

Definition (non-quantized case)

For a given continuous object $S \subset \mathbb{R}^2$, inscribed into an integer grid with pixels $p_{(i,j)}$, the *pixel coverage digitization* of S is

$$\mathcal{D}(S) = \left\{ \left((i,j), \frac{A(p_{(i,j)} \cap S)}{A(p_{(i,j)})} \right) \middle| (i,j) \in \mathbb{Z}^2 \right\} ,$$

where $A(X)$ denotes the area of a set X.

Digital images $\rightarrow$ Quantized grey values

Definition (n-level quantized case)

$$\mathcal{D}^n(S) = \left\{ \left((i,j), \frac{1}{n} \left\lfloor n \frac{A(p_{(i,j)} \cap S)}{A(p_{(i,j)})} + \frac{1}{2} \right\rfloor \right) \middle| (i,j) \in \mathbb{Z}^2 \right\} ,$$

where $\lfloor x \rfloor$ denotes the largest integer not greater than x.

Pixel coverage digitization

The membership value of a pixel is
equal to its relative coverage by the digitized object:

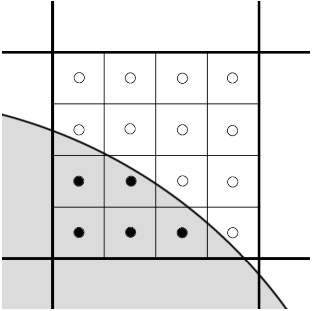

Example: Pixel coverage approximated by super sampling;

$$\alpha_1 = \frac{5}{16}, \ \alpha_2 = \frac{11}{16}.$$

Pixel coverage segmentation

We have proposed five segmentation methods which provide (approximate) pixel coverage images:

1. Direct assignment of area coverage values from a continuous segmentation model.
   - A. Tanács, C. Domokos, N. Sladoje, J. Lindblad, and Z. Kato. Recovering affine deformations of fuzzy shapes. SCIA 2009. LNCS-5575, pp. 735–744, 2009.
2. A method based on mathematical morphology and a double thresholding scheme.
   - N. Sladoje and J. Lindblad. High Precision Boundary Length Estimation by Utilizing Gray-Level Information. IEEE Trans. on PAMI, Vol. 31, No. 2, pp. 357–363, 2009.
3. A method providing local sub-pixel classification extending any existing crisp segmentation.
   - N. Sladoje and J. Lindblad. Pixel coverage segmentation for improved feature estimation. ICIAP 2009. LNCS-5716, pp. 929-938, 2009.
4. A framework (and methods) for coverage segmentations of graphs.
   - F. Malmberg, J. Lindblad, I. Nyström. Sub-pixel segmentation with the image foresting transform. IWCIA 2009. LNCS-5852, pp. 201–211, 2009.
   - F. Malmberg, J. Lindblad, N. Sladoje, I. Nyström. A Graph-based Framework for Sub-pixel Image Segmentation. Theoretical Comput. Sci. Vol 412, No 15, pp. 1338–1349, 2011.
5. Method based on energy minimization of a Mumford-Shah style functional.
   - J. Lindblad and N. Sladoje. Coverage Segmentation based on Linear Unmixing and Minimization of Perimeter and Boundary Thickness. Submitted.

Pixel coverage segmentation

Definition (pixel coverage segmentation)

A *pixel coverage segmentation* of an image I into m components $c_k, k \in \{1, 2, \ldots, m\}$ is

$$\mathcal{S}(I) = \left\{ \left((i,j), \alpha_{(i,j)} \right) \,\middle|\, (i,j) \in I_D \right\} \ ,$$

where

$$\alpha_{(i,j)} = (\alpha_1, \ldots, \alpha_m) \, , \ \sum_{k=1}^{m} \alpha_k = 1 \, , \quad \alpha_k = \frac{A(p_{(i,j)} \cap S_k)}{A(p_{(i,j)})} \ ,$$

and where $S_k \in \mathbb{R}^2$ is the extent of the component c_k and $I_D \subseteq \mathbb{Z}^2$ is the image domain.

The sets S_k are, in general, not known, and the values α_k have to be estimated from the image.

Method 3: Un-mixing based on local classification

Assumption

Partial pixel coverage exist only at the object boundaries of an existing crisp segmentation.

Approach

Re-assign class belongingness to the boundary pixels based on a local classification using the surrounding non-boundary pixels.

To obtain a pixel coverage segmentation, we propose a method composed of the following four steps:

1. Application of a crisp segmentation method, appropriately chosen for the particular task
2. Selection of pixels to be assigned partial coverage
3. Application of a liner mixture model for “de-mixing” of partially covered pixels and assignment of pixel coverage values
4. Ordered thinning of the set of partly covered pixel to provide one pixel thin 4-connected regions of mixed pixels

Steps 1 and 2.

1. **Any** crisp segmentation model.
   - For the example to come, we used Linear Discriminant Analysis in combination with Iterated Relative Fuzzy Connectedness[1]

2. **Selection of pixels to re-evaluate**
   - All pixel which are 4-connected to a pixel with a different label.

[1] J. Lindblad, N. Sladoje, V. Ćurić, H. Sarve, C.B. Johansson, and G. Borgefors. Improved quantification of bone remodelling by utilizing fuzzy based segmentation. SCIA 2009

3. Computation of partial pixel coverage values

3.1 Estimate the spectral properties c_k of the pure classes locally.

- The mean values of the respective classes present in the assumed **completely covered** pixels in a local Gaussian neighbourhood.

3.2 Compute the mixture proportions a_k of the pixels selected in step 2.

- The intensity values of a mixed pixel $p = (p_1, p_2, \ldots, p_n)$ (n being the number of channels of the image) are assumed, in a noise-free environment, to be a convex combination of the pure classes c_k:

$$p = \sum_{k=1}^{m} \alpha_k c_k \,, \quad \sum_{i=k}^{m} \alpha_k = 1 \,, \quad \alpha_k \geq 0 \,. \qquad (1)$$

where each coefficient α_k corresponds to the coverage of the pixel p by an object of a class c_k.

3. Computation of partial pixel coverage values

In the presence of noise, it is not certain that there exists a (convex) solution to the linear system (1). Therefore we reformulate the problem as follows:

Find a point p^* of the form $p^* = \sum_{k=1}^{m} \alpha_k^* c_k$, such that p^* is a *convex* combination of c_k and the distance $d(p, p^*)$ is minimal. We solve the constrained optimization problem by using Lagrange multipliers, and minimize the function

$$F(\alpha_1, \ldots, \alpha_m, \lambda) = \|p - \sum_{k=1}^{m} \alpha_k c_k\|_2^2 + \lambda(\sum_{k=1}^{m} \alpha_k - 1)$$

over all $\alpha_k \geq 0$. This leads to a least squares type of computation.

The obtained solution provides estimated partial coverage of the pixel p by each of the observed classes c_k.

4. Ordered thinning

To ensure one pixel thick boundaries, the “least” mixed pixels are one at a time assigned to their most prominent class, until only one pixel thick mixed boundaries remain.

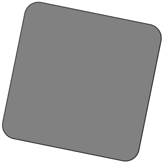

(a) Test object

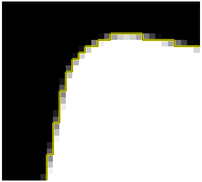

(b) Part of pixel coverage segm.

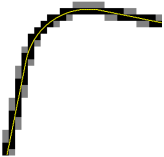

(c) Part of re-evaluated set

Some features that benefit from a pixel coverage representation.

Area and other geometric moments

- N. Sladoje and J. Lindblad. Estimation of Moments of Digitized Objects with Fuzzy Borders. ICIAP'05, LNCS-3617, pp. 188-195, Cagliari, Italy, Sept. 2005.

$$m_{p,q}(S) = \frac{1}{r^{p+q+2}}\,\tilde{m}(rS) + \mathcal{O}\left(\frac{1}{r\sqrt{n}}\right)$$

Perimeter and boundary length

- N. Sladoje and J. Lindblad. High Precision Boundary Length Estimation by Utilizing Gray-Level Information. IEEE Trans. on PAMI, Vol. 31, No. 2, pp. 357-363, 2009.

$$\gamma_n^{(0,q)} = \frac{2q}{q + \sqrt{(\sqrt{n^2+q^2} - n)^2 + q^2}}\,, \quad |\varepsilon_n| = \mathcal{O}(n^{-2})$$

Signature

- J. Chanussot, I. Nyström and N. Sladoje, Shape signatures of fuzzy star-shaped sets based on distance from the centroid, Pattern Recognition Letters, vol. 26(6), pp. 735-746, 2005.

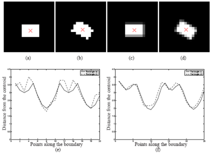

Perimeter estimation

Formulation of the problem:

Having a **discrete representation** of a real object, digitized in an integer grid, **estimate** its perimeter (length of its border) with as small error as possible.

We wish to obtain as correct feature values as possible - **accuracy**, and that repeated measurements provide similar results - **precision**.

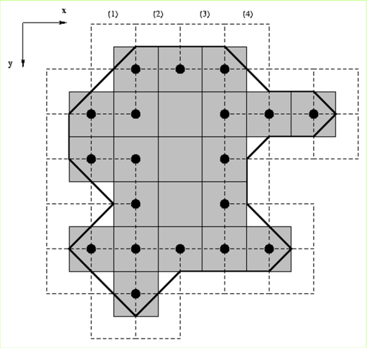

One approach

Local polygonalization
Approximate the object perimeter with the perimeter of a locally defined polygon.

Direct use of the perimeter of the polygon gives, on average, an **overestimate**.

How to assign local step lengths

Using 4 edge directions.

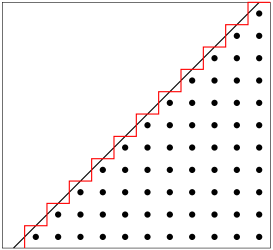

Digital edge $\sqrt{2}$ times longer than true edge.

Using 8 edge directions.

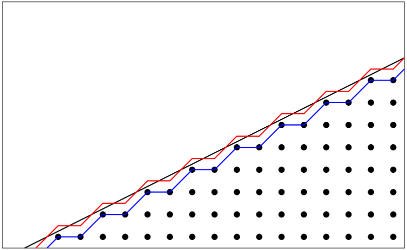

Edge 1.08 times longer than true edge.

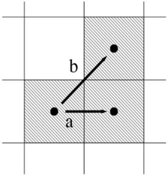

Freeman 1970:
$a = 1, \quad b = \sqrt{2}$

Using $a = 1$, $b = \sqrt{2}$ lead to an **overestimate**.

Error minimization

Verwer 1991

- Decide what error to minimize
  - The mean square error (MSE) minimization leads to estimators that, in average, perform well for lines of all directions.
  - The maximal error minimization leads to estimator with a better "controllable" error.
- Compute **optimal step lengths** to minimize the chosen error measure when estimating the length of straight segments of arbitrary direction.

- To minimize MSE: $a = 0.9481$ and $b = 1.3408$. Root Mean Square (RMS) Error is 2.33%.
- To minimize MaxErr: $a = 0.9604$ and $b = 1.3583$. Maximal Error is 3.95%.
- **The error does not decrease with increasing resolution**

The straight edge of a halfplane

Discrete, grey-scale, non-quantized

Observe a halfplane $H = \{(x,y) \mid y(x) \leq kx + m,\ k,m \in [0,1]\}$, over an interval $x \in [0,N]$, $N \in \mathbb{Z}^+$.
Let I be the non-quantized pixel coverage digitization $I = \mathcal{D}(H)$ ($\Delta x = \Delta y = h = 1$ by definition.)

Then it holds that

$$y(i) = \sum_{j \geq 0} I(i,j) - 0.5$$

$$k(i) = y(i+1) - y(i) = k$$

$$l = \sqrt{N^2 + (kN)^2} = \sum_{i=0}^{N-1} \sqrt{1 + k(i)^2}$$

The length of the edge segment l is "estimated" with **no error**.

Non-quantized example

$l = 4.39$

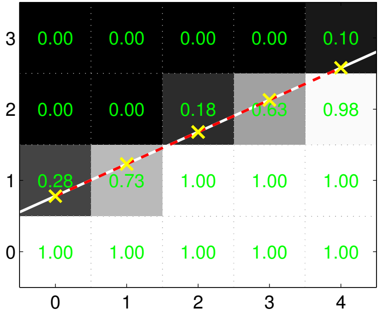

s_c:	1.28		1.73		2.18		2.63		3.08
d_c:		0.45		0.45		0.45		0.45	
l_c:		1.10		1.10		1.10		1.10	

Figure: Example illustrating edge length estimation based on the difference d_c of column sums s_c for a segment ($N = 4$) of a halfplane edge given by $y \leq 0.45x + 0.78$.

$$s_c = \sum_{j \geq 0} I(c,j) \ , \ d_c = s_{c+1} - s_c \ , \ l_c = \sqrt{1 + d_c^2}$$

The straight edge of a halfplane

Discrete, grey-scale, quantized

Observe a halfplane $H = \{(x,y) \mid y(x) \le kx + m,\ k,m \in [0,1]\}$, over an interval $x \in [0,N]$, $N \in \mathbb{Z}^+$.
Let I be the **quantized** pixel coverage digitization $I = \mathcal{D}^n(H)$

Then

$$\tilde{l} = \sum_{c=0}^{N-1} \sqrt{1 + d_c^2}$$

provides an estimate of the edge length l.

However, this is in general an overestimate (zig-zag steps).
Scaling the estimate with an optimally chosen factor $\gamma_n < 1$, gives an estimate with a minimal error.

$$\hat{l} = \sum_{c=0}^{N-1} \gamma_n \sqrt{1 + d_c^2}$$

Quantized example

$$\hat{l} = \gamma_5 * 4.49$$

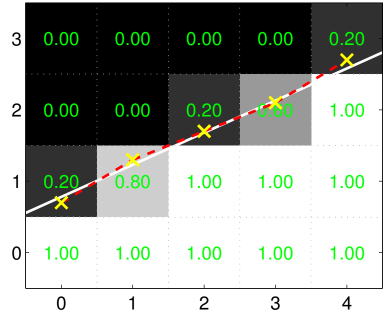

$\tilde{s}_c$:	1.20		1.80		2.20		2.60		3.20
$\tilde{d}_c$:		0.60		0.40		0.40		0.60	
$\tilde{l}_c$:		1.17		1.08		1.08		1.17	

Figure: Example illustrating edge length estimation based on the difference d_c of column sums s_c for a segment ($N = 4$) of a halfplane edge given by $y \leq 0.45x + 0.78$.

$$s_c = \sum_{j \geq 0} I(c, j) \ , \ d_c = s_{c+1} - s_c \ , \ l_c = \sqrt{1 + d_c^2}$$

Minimization of the maximal relative error

Result [Sladoje and Lindblad, PAMI 2009]

The maximal error is minimized for

$$\gamma_n^q = \frac{2q}{q + \sqrt{(\sqrt{n^2+q^2} - n)^2 + q^2}}, \text{ where } q = j - i\,.$$

The maximal error is $|\varepsilon| = 1 - \gamma_n^q$.
Quantization leads to $q > 1$. In 2D it holds that $q \leq 3$.

Asymptotic behaviour

Observing the estimation error as a function of the number of grey-levels n, we conclude that

$$|\varepsilon_n| = \mathcal{O}\left(\frac{1}{n^2}\right) .$$

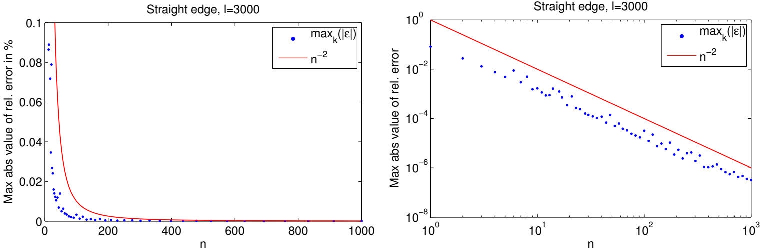

(a) lin-lin scale (b) log-log scale

Figure: Asymptotic behaviour of the maximal error for straight edge length estimation using $\gamma_n = \gamma_n^1$; theoretical (line) and empirical (points) results.

Assignment of a length to a segment

For lines of a slope $k \in [0, 1]$, each value d_c depends on at most six pixels, located in a 3×2 rectangle:

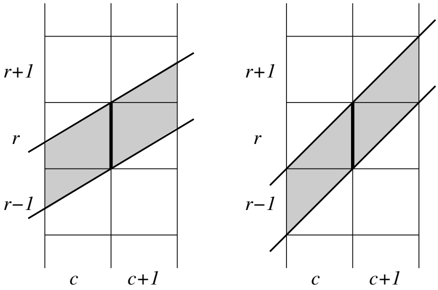

(a) $k = 0.6$ (b) $k = 1$

Figure: Regions where lines $y = kx + m$ with k, m such that $r - \frac{1}{2} \leq u = k(c + \frac{1}{2}) + m \leq r + \frac{1}{2}$, intersect a 3×2 configuration.

Assignment of a length to a segment - local conditions

Analytically defined half-plane

A condition to be checked for a 3×2 neighbourhood of a pixel $p_{(c,r)}$ in continuous case is

$$r - \frac{1}{2} \leq u = k(c + \frac{1}{2}) + m \leq r + \frac{1}{2},$$

for a line $y = kx + m$

Locally observed discretized half-plane

In a discrete case, $u = k(c + \frac{1}{2}) + m$ is **estimated** by

$$\tilde{u} = r - \frac{3}{2} + \frac{1}{2} \sum_{i=1}^{6} \tilde{p}_i$$

and the same condition

$$r - \frac{1}{2} \leq \tilde{u} \leq r + \frac{1}{2}$$

is used.

Local contributions calculations

Local contributions to the length of a segment

A local length assigned to a 3×2 neighbourhood of a pixel $p_{(c,r)}$ is

$$\tilde{l}^{D}_{(c,r)} = \begin{cases} \sqrt{1 + d^2_{(c,r)}}\,, & \tilde{u} \in \left(r - \frac{1}{2}, r + \frac{1}{2}\right) \\ \frac{1}{2}\sqrt{1 + d^2_{(c,r)}}\,, & \tilde{u} = r \pm \frac{1}{2} \\ 0\,, & \text{otherwise}\,. \end{cases}$$

Isometries of the plane - cases when $|k| \notin [0, 1]$

- If $|k| \notin [0, 1]$, we need 2×3 configuration to estimate the slope; when we exchange roles of the axes, we can apply the same algorithms as for the former case.
- Instead of changing size of configuration depending on k, we use 3×3 configurations in all cases.
- Apply isometric transformations to the 3×3 to make $|k| \in [0, 1]$.

Algorithm

Input: Pixel coverage values $\tilde{p}_i,\ i = 1, \ldots, 9$, from a 3×3 neighbourhood $T_{(c,r)}$.
Output: Local edge length $\hat{l}^T_{(c,r)}$ for the given 3×3 configuration.

---

if $\tilde{p}_7 + \tilde{p}_8 + \tilde{p}_9 < \tilde{p}_1 + \tilde{p}_2 + \tilde{p}_3$ /* $y \geq kx + m$ */
  swap$(\tilde{p}_1, \tilde{p}_7)$
  swap$(\tilde{p}_2, \tilde{p}_8)$
  swap$(\tilde{p}_3, \tilde{p}_9)$
endif

if $\tilde{p}_3 + \tilde{p}_6 + \tilde{p}_9 < \tilde{p}_1 + \tilde{p}_4 + \tilde{p}_7$ /* $k < 0$ */
  swap$(\tilde{p}_1, \tilde{p}_3)$
  swap$(\tilde{p}_4, \tilde{p}_6)$
  swap$(\tilde{p}_7, \tilde{p}_9)$
endif

if $\tilde{p}_4 + \tilde{p}_7 + \tilde{p}_8 < \tilde{p}_2 + \tilde{p}_3 + \tilde{p}_6$ /* $k > 1$ */
  swap$(\tilde{p}_2, \tilde{p}_4)$
  swap$(\tilde{p}_3, \tilde{p}_7)$
  swap$(\tilde{p}_6, \tilde{p}_8)$
endif

$\tilde{s}_1 = \tilde{p}_1 + \tilde{p}_4 + \tilde{p}_7$
$\tilde{s}_2 = \tilde{p}_2 + \tilde{p}_5 + \tilde{p}_8$
$\tilde{s}_3 = \tilde{p}_3 + \tilde{p}_6 + \tilde{p}_9$

$\tilde{u}_l = (\tilde{s}_1 + \tilde{s}_2)/2$
$\tilde{u}_r = (\tilde{s}_2 + \tilde{s}_3)/2$

if $1 \leq \tilde{u}_l < 2$
  $\tilde{d}_l = \tilde{s}_2 - \tilde{s}_1$
  $\hat{l}_l = \frac{\gamma_n}{2}\sqrt{1 + \tilde{d}_l^2}$
else
  $\hat{l}_l = 0$
endif

if $1 < \tilde{u}_r \leq 2$
  $\tilde{d}_r = \tilde{s}_3 - \tilde{s}_2$
  $\hat{l}_r = \frac{\gamma_n}{2}\sqrt{1 + \tilde{d}_r^2}$
else
  $\hat{l}_r = 0$
endif

$\hat{l}^T_{(c,r)} = \hat{l}_l + \hat{l}_r$

Only **integer arithmetics** used locally (fast, exact).
Only **local** information is used (fast, stable, parallelizable).

Perimeter estimation errors

Trade-off between spatial and grey-level resolution

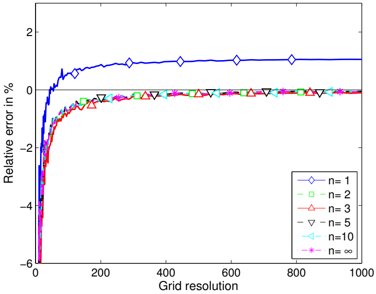

(a) lin-lin scale

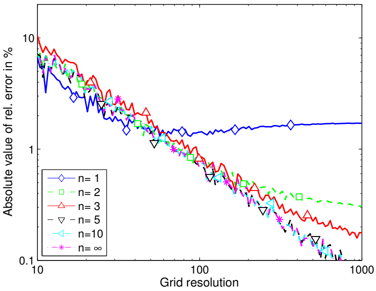

(b) log-log scale

Figure: Relative errors in percent for test shapes digitized at increasing resolution for 5 different quantization levels and non-quantized ($n = \infty$).

Segm. (method 2) + perimeter estimation

Digital photos of the straight edge of a white paper on a black background at a number of angles using a Panasonic DMC-FX01 digital camera in grey-scale mode.

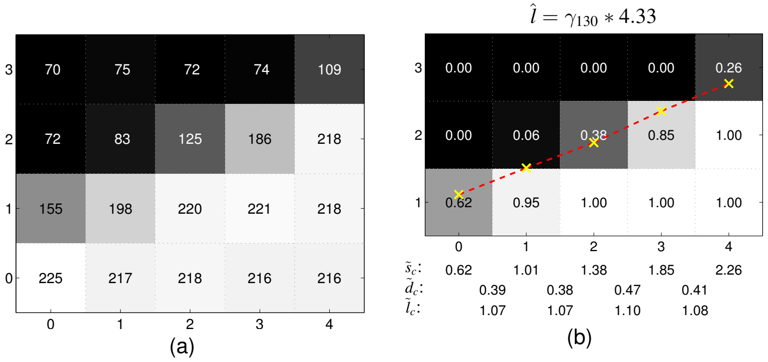

Figure: (a) Close up of the straight edge of a white paper imaged with a digital camera. (b) Segmentation output from Algorithm 2 using 130 positive grey-levels. Approximating edge segments are superimposed.

Results – Segm. method 2 + perimeter est.

The observed noise range in the images is between 20 and 50 grey-levels, out of 255, and the found value of n in the segmentation varies from 90 to 140 for the different photos.

The observed maximal errors for the methods are as follows:

- Proposed method **0.14%**;
- Binary 3.95%;
- Corner count 1.61%;
- Eberly & Lancaster 8.78%;
- Gauss $\sigma = 2$ + E & L 0.57%;
- Gauss $\sigma = 4$ + E & L 0.58%.

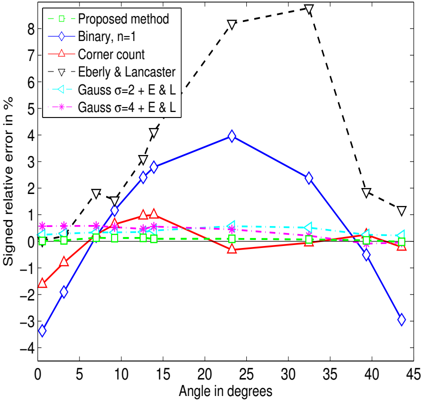

Segm. 3 + coverage,perimeter,area

Synthetic data with added noise

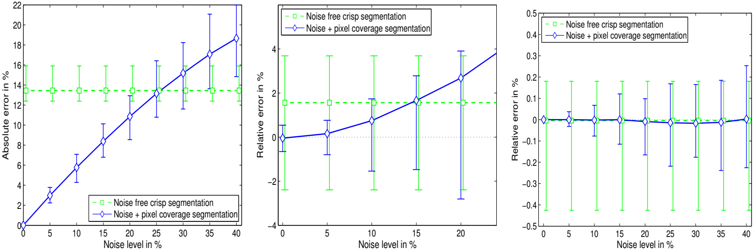

(a) Coverage values (b) Perimeter estimate (c) Area estimate

Figure: Estimation errors for increasing levels of noise. Green is noise free crisp reference. Bars represent max and min.

Segm. method 5 Energy minimization

Segmentation formulated as an energy minimization problem:

$$J(A) = D(A) + \mu P(A) + \nu T(A) + \xi F(A) \ ,$$

where $D(A), P(A), T(A), F(A)$ are **data term, overall perimeter, boundary thickness, and total image fuzziness**, and where $\mu, \nu, \xi \geq 0$ are weighting parameters,

The sought coverage segmentation A^* is obtained by minimizing J over the set of coverage segmentations>

$$A^* = \arg\min_A J(A). \tag{2}$$

Being able to differentiate the energy functional J, we can utilize powerful numerical optimization methods. We used the Spectral Projected Gradient method.

Segm. method 5 Energy minimization

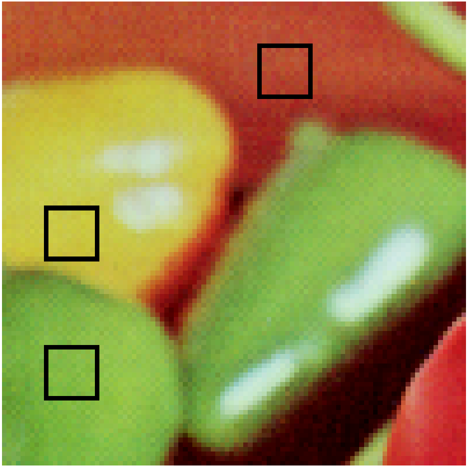

Figure: Example colour image with three square training regions.

Segm. method 5 Energy minimization

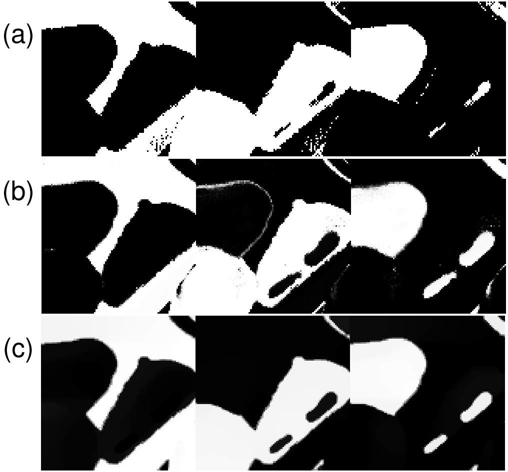

Figure: (a) Segmentation obtained by linear discriminant analysis. (b) Segmentation obtained by fuzzy c-means clustering. (c) Segmentation obtained by energy minimization.

High resolution reconstruction disk vs. octagon

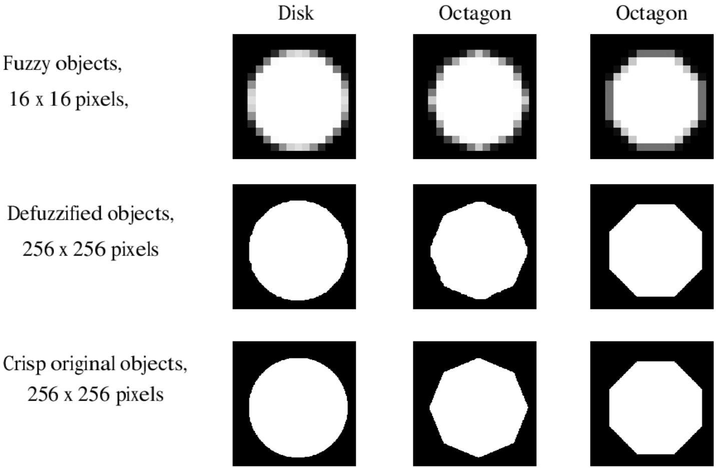

Application 1

Affine registration of digital X-ray images of hip-prosthesis implants for follow up examinations

Segmentation method 1, using active contours (snakes), modified to provide pixel coverage values utilized for improved moments' estimation in the registration process.

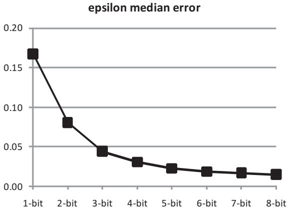

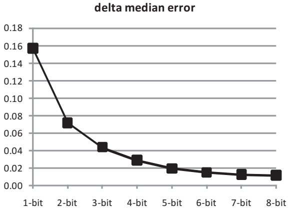

Registration results of 2000 synthetic images using different quantization levels of the fuzzy boundaries.

Application 1

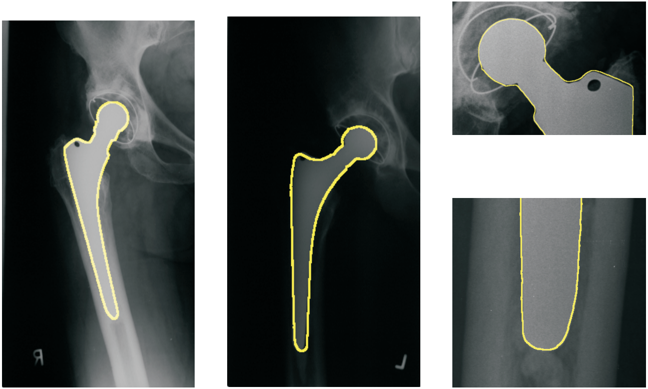

$\delta = 2.17\%$ $\delta = 4.81\%$ $\delta = 1.2\%$

Figure: Real X-ray registration results. (a) and (b) show full X-ray observation images and the outlines of the registered template shapes. (c) shows a close up view of a third study around the top and bottom part of the implant.

Application 2

Measure bone implant integration for the purpose of evaluating new surface coatings which are stimulating bone regrowth around the implant.

Segmentation method 3, area and boundary estimates.

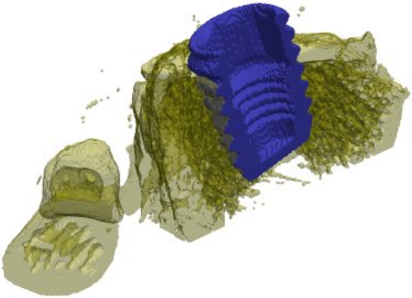

Application 2

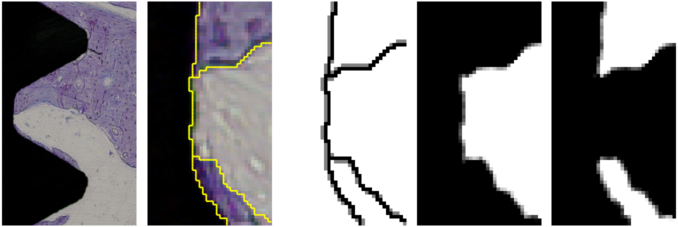

(a) (b) (c) (d) (e)

Figure: (a): The screw-shaped implant (black), bone (purple) and soft tissue (light grey). (b) Part of a crisp (manual) segmentation of (a). (c) The set of re-evaluated pixels. (d) and (e) Pixel coverage segmentations of the soft tissue and the bone region, respectively.

Result:

Approximately a **30% reduction of errors** on average, as compared to when using estimates from the crisp starting segmentation.

Application 3

User assisted segmentation of the spleen, for medical diagnosis based on accurate feature estimates. Method 4, area est.

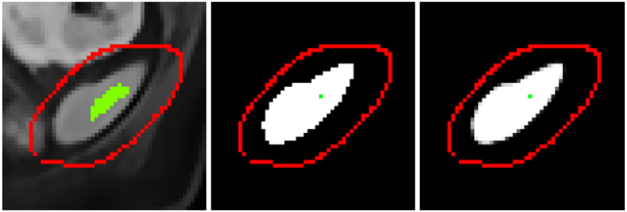

Fig. 3. Segmentation of the spleen in a slice from a CT volume.(Left) Seed-point regions used in the experiment. The green pixels define all object seeds, while the red pixels define background seeds. Single pixels from the green region were used to define object seeds. (Middle) Example result of crisp IFT. (Right) Example result of the proposed sub-pixel IFT.

Table 1. Statistics on the measured area for the 41 segmentations in the experiment. (Areas are given in number of pixels.)

Method	Mean area	Min area	Max area	σ
Crisp IFT	266.5	265	269	0.98
Sub-Pixel IFT	266.2	265.4	266.7	0.40

Result: 50% reduction of standard deviation of estimates, as compared to when using estimates from the crisp starting segmentation.

Application 3

User assisted segmentation of the spleen, for medical diagnosis based on accurate feature estimates.

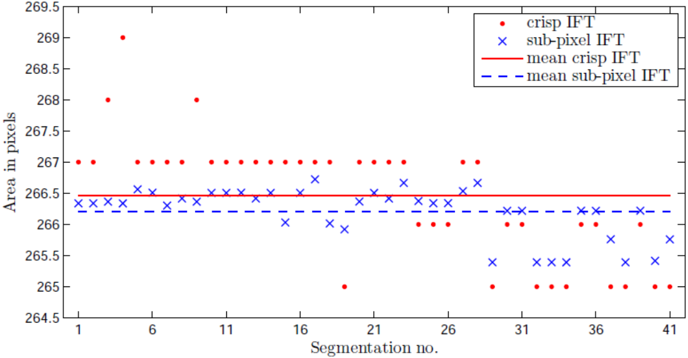

Result: Assuming that the mean result is correct, **more than 3 times reduction of the maximal error**, as compared to when using estimates from the crisp starting segmentation.

Conclusions

- Pixel coverage representations are shown to be **superior** to crisp image object representations for many reasons.
- By suitably utilizing information available in images it is possible to perform a **Pixel coverage segmentation**.
- It is relatively easy to extend **any** existing crisp segmentation to a coverage segmentation.
- We observe that even for moderate amount of noise, the achieved pixel coverage representation provides a **more accurate** representation of image objects than a perfect, noise free, crisp representation.
- For a number of shape features, **significant performance improvement** is shown, both theoretically and empirically.
- More research work remains! :-)

Thanks to the people involved

- Dr. Nataša Sladoje
- Filip Malmberg
- Hamid Sarve
- Vladimir Ćurić
- Dr. Attila Tanács
- Csaba Domokos
- Prof. Zoltan Kato
- Prof. Gunilla Borgefors
- Prof. Carina Johansson
- Prof. Jocelyn Chanussot
- Doc. Ingela Nyström
- Prof. Joviša Žunić